JOURNAL OF VIROLOGY, May 2009, p. 4262–4274 Vol. 83, No. 9
0022-538X/09/$08.00+0 doi:10.1128/JVI.00021-09

Components of Nuclear Domain 10 Bodies Regulate Varicella-Zoster Virus Replication▽

Christos A. Kyratsous and Saul J. Silverstein*

Department of Microbiology, College of Physicians and Surgeons, Columbia University, 701 W. 168th St., New York, New York 10032

Received 5 January 2009/Accepted 4 February 2009

PML, Sp100, and Daxx are proteins that normally reside within nuclear domains 10 (ND10s). They associate with DNA virus genomes and repress the very early stages of the DNA virus replication cycle. Virus-encoded proteins counteract this innate antiviral response. ICP0, a herpes simplex virus (HSV) immediate-early protein, is necessary and sufficient to dissociate ND10s and target their two major components, PML and Sp100, for proteasomal degradation. In this report, we show that ORF61p, the varicella-zoster virus (VZV) ortholog of ICP0, does not degrade PML and alters Sp100 levels only slightly. Furthermore, we demonstrate that other virus proteins cannot substitute for this lack of function during infection. By using short interfering RNAs, we depleted PML, Sp100, and Daxx and studied their roles in plaquing efficiency, virus protein accumulation, infectious-center titer, and virus spread. The results of these studies show that components of ND10s can accelerate VZV replication but do not ultimately control cell-associated virus titers. We conclude that while both ICP0 and ORF61p activate virus gene expression, they modulate host innate repression mechanisms in two different ways. As a result, HSV and VZV commandeer their host cells by distinct mechanisms to ensure their replication and spread.

Nuclear domains 10 (ND10s), also known as promyelocytic leukemia protein (PML) nuclear bodies and PML oncogenic domains, are dynamic macromolecular inclusions of cellular proteins that form within the interchromosomal space in the nucleus (2, 65). The sizes and frequencies of these bodies range from 0.2 to 1 μm and 2 to 30 per cell, depending on the cell type and the stage of the cell cycle (2, 17, 62). Cellular proteins that accumulate at these sites are divided into two groups: proteins that are permanent components, such as PML, Sp100 (speckled protein of 100 kDa), Daxx, SUMO-1, and the Bloom syndrome helicase BLM, and proteins that associate with ND10s only under specific conditions (e.g., DNA repair machinery) or during overexpression (e.g., BRCA1) (69).

DNA virus genomes associate with ND10 components at the initial stages of their replication cycles. Newly formed transcription and replication sites localize close to proteins that normally reside within ND10s (61). The first suggestion that virus replication affects ND10s was the demonstration that PML staining disappears after herpes simplex virus (HSV) infection (46). Subsequently, parental genomes of herpesviruses, adenoviruses, simian virus 40, and papillomaviruses were shown to be associated with ND10s (10, 14, 32, 33, 35, 47).

The antagonistic relationship between HSV and components of ND10s has been extensively studied. The expression of ICP0, a viral protein, is required and sufficient for the destruction of the nuclear structure (18, 45, 46). ICP0 is a C_3HC_4 RING finger-containing nuclear phosphoprotein with an apparent molecular mass of 110 kDa (56) that behaves as a promiscuous activator of both viral and cellular genes (12, 23, 59). Virus mutants lacking the ICP0 gene have increased particle-to-PFU ratios, substantially lower yields, and decreased levels of α gene expression (13, 64). ICP0 also functions as an E3 ubiquitin ligase to target a growing list of host proteins, including components of ND10 bodies such as the SUMO-1-modified forms of PML and Sp100, for proteasomal degradation (8, 15, 18, 26, 41, 53).

HSV mutants that fail to express ICP0 are defective in their abilities to modify and degrade ND10 components (46). The depletion of PML and Sp100 accelerates virus gene expression and increases plaquing efficiency for HSV ICP0-defective mutants but has no effect on wild-type virus. These data show that PML and Sp100 are components of an intrinsic anti-HSV defense mechanism that is counteracted by ICP0's E3 ligase activity to ensure efficient virus replication and growth (21, 22).

Varicella-zoster virus (VZV) is a common human pathogen that is classified together with HSV as an alphaherpesvirus. VZV encodes an ICP0 ortholog (ORF61p) (49, 57) that, similar to ICP0, transcriptionally activates viral promoters and enhances the infectivity of viral DNA (49, 50). Importantly, ORF61p contains a RING finger domain, homologous to the one that is essential for ICP0's transactivation and ND10 dissociation and degradation activities.

We have shown previously that the expression of ICP0 by HSV is required to overcome the depletion of BAG3, a host cochaperone protein that stimulates virus gene expression and protein accumulation (38). Although ORF61p is considered to be functionally similar to ICP0 (49), VZV is affected by the depletion of BAG3 (37), suggesting that ICP0 and ORF61p have evolved separately to provide different functions for virus replication.

In this report, we demonstrate that ORF61p or other VZV-encoded proteins do not degrade ND10 components in the same manner as ICP0 in HSV-infected cells. We have also studied the roles of PML, Sp100, and Daxx during VZV infec-

* Corresponding author. Mailing address: Department of Microbiology, College of Physicians and Surgeons, Columbia University, 701 W. 168th St., New York, NY 10032. Phone: (212) 305-8149. Fax: (212) 305-5106. E-mail: sjs6@columbia.edu.

▽ Published ahead of print on 11 February 2009.

tion and highlight key differences in the two related alphaherpesviruses HSV and VZV.

MATERIALS AND METHODS

Mammalian cells. Human melanoma (MeWo), siBAG3 (37), siPML (38), and 293A cells were maintained as described previously (37).

To generate stable cell lines expressing small interfering RNAs (siRNAs) targeting Sp100 and Daxx mRNAs, MeWo cells were infected with retroviruses and selected in growth medium containing 200 and then 500 μg/ml hygromycin, resulting in the cell lines siSp100 and siDaxx.

Transformation with DNA. The appropriate cell lines were transformed with DNA by using Fugene HD (Roche, Indianapolis, IN).

Drug treatment. Alpha interferon was purchased from PBL Biomedical (Piscataway, NJ).

Viruses. (i) VZV. VZV Jones, a wild-type clinical isolate, was propagated and titrated as described previously (24). Cell-free virus was prepared as described previously (36, 58).

(ii) Retroviruses. Retroviruses were constructed by the transient cotransformation of 293T cells with the proviral vectors pCK-Super.retro.hygro (38), pCK-siSp100 or pCK-siDaxx and pgag-polgpt (44), and pHCMV-G (74).

(iii) Adenoviruses. Adenoviruses Adempty, AdICP0, and AdORF61 were described previously (73, 75).

Virus growth assays. (i) Plaque assays. MeWo, siPML, siSp100, or siDaxx cells were infected with 10-fold serial dilutions of virus stocks, infected cells were fixed and stained, and plaques were counted.

(ii) Growth curves. The titer of cell-associated VZV after the infection of MeWo, siPML, siSp100, or siDaxx cells was determined by mixing infected cells with uninfected MeWo cells and counting the resulting plaques after fixing and staining.

siRNA plasmid construction. Previously described siRNA oligonucleotides targeting Sp100 and Daxx mRNAs (22, 68) were modified for cloning into pCK-super.retro.hygro (38). To generate pCK-siSp100 and pCK-siDaxx, the following annealed oligonucleotide pairs were ligated into BglII/HindIII-cleaved pCK-super.retro.hygro (38): siSp100_upper (5′-GATCCCCGTGAGCCTGTGATCAATAATTCAAGAGATTATTGATCACAGGCTCACTTTTTA-3′) and siSp100_lower (5′-AGCTTAAAAAGTGAGCCTGTGATCAATAATCTCTTGAATTATTGATCACAGGCTCACGGG) and siDaxx_upper (5′-GATCCCCGGAGTTGGATCTCTCAGAATTCAAGAGATTCTGAGAGATCCAACTCCTTTTTA-3′) and siDaxx_lower (5′-AGCTTAAAAAGGAGTTGGATCTCTCAGAATCTCTTGAATTCTGAGAGATCCAACTCCGGG-3′).

All primers were obtained from Operon Biotechnologies (Huntsville, AL), and all vector inserts were verified by DNA sequencing.

Antibodies. Rabbit polyclonal antibodies against amino acids (aa) 1086 to 1201 of ORF29p and aa 1 to 265 of ORF63p were described previously (43).

Polyclonal antibodies to ICP0 have been described previously (40). Monoclonal ICP0 and ORF62p antibodies were purchased from the Rumbaugh-Goodwin Institute (Plantation, FL). Polyclonal antibodies against a glutathione *S*-transferase fusion protein containing aa 136 to 248 of ORF61p were raised in rabbits and purified by affinity chromatography as described before (37). Monoclonal antibodies to PML, GAPDH (glyceraldehyde-3-phosphate dehydrogenase), and tubulin and polyclonal antibodies to Daxx were from Santa Cruz Biotechnology (Santa Cruz, CA). Polyclonal antibodies against PML and Sp100 were purchased from Chemicon (Temecula, CA). Antibodies to STAT1, STAT2, and phosphorylated STAT1 were from Abcam (Cambridge, MA). Antibodies against phosphorylated STAT2 were purchased from Santa Cruz Biotechnology.

Alexa Fluor 488-conjugated anti-mouse and Alexa Fluor 546-conjugated anti-rabbit antibodies were from Molecular Probes (Carlsbad, CA). Goat anti-rabbit and anti-mouse antibodies conjugated to horseradish peroxidase for immunoblotting were from KPL (Gaithersburg, MD).

Indirect immunofluorescence microscopy. Cells on glass coverslips were fixed and stained with antibody and Hoechst as described previously (37). All samples were visualized with an Axiovert 200 M inverted microscope (Carl Zeiss Microimaging Inc., Thornwood, NY), and images were acquired with a model no. C4742-80-12AG digital charge-coupled device camera (Hamamatsu Photonics, Hamamatsu-City, Japan) using Openlab 5 software (Improvision, Lexington, MA). Images were deconvolved using Openlab 5 and assembled in Photoshop CS3 (Adobe Systems, San Jose, CA).

SDS-PAGE and Western blotting. Infected or biochemically transformed cells were washed twice with cold phosphate-buffered saline (PBS) and lysed in 1.5× sodium dodecyl sulfate (SDS) sample buffer (75 mM Tris-HCl, pH 6.8, 150 mM dithiothreitol, 3% SDS, 0.15% bromophenol blue, 15% glycerol), the lysates were boiled, and the proteins were analyzed by SDS-polyacrylamide gel electrophoresis (PAGE) (39). Proteins were transferred onto nitrocellulose membranes before Western blotting. After the membranes were blocked in 5% nonfat milk in PBS–0.1% Tween 20 (PBST), immobilized proteins were allowed to react with the appropriate antibodies in 1% nonfat milk in PBST. Membranes were washed three times for 5 min each with PBST, incubated with an anti-rabbit or anti-mouse antibody conjugated to horseradish peroxidase, and washed again three times for 5 min each with PBST and twice with PBS for 5 min each. Antibodies were visualized by the addition of LumiGLO substrate (KPL) and exposure to X-ray film.

When the antibodies against the STAT proteins were used, blocking and antibody incubations were performed with PBST supplemented with 50 mM NaF, 1 mM Na_3VO_4, and 3% bovine serum albumin.

Sequence alignment. The amino acid sequences of ORF61p (accession number NP_040183.1) and ICP0 (accession number NP_044601.1) were aligned with MacVector version 10.0 (MacVector Inc., Cary, NC) using the Gonnet matrix, an open-gap penalty of 10.0, and an extend-gap penalty of 0.1.

RESULTS

Sequence similarities between ICP0 and ORF61p. Previous reports suggested that the alphaherpesvirus orthologs ICP0 and ORF61p share several biological features, including their abilities to function as activators of gene expression and enhancers of viral DNA infectivity (49, 50, 57). However, we have reported that unlike ICP0, ORF61p does not substitute for the loss of BAG3 during virus infection, suggesting that these proteins do not serve identical functions in their native contexts (38). Multiple functions of ICP0 have been mapped to specific domains (16). We thus hypothesized that the alignment of the amino acid sequences of these proteins might provide insight into their differences.

The amino acid sequences of ICP0 and ORF61p (accession numbers NP_044601.1 and NP_040183.1, respectively) were retrieved from the NCBI protein database and aligned (Fig. 1). Despite some conservation of the corresponding nucleotide sequences (9), there is little overall amino acid conservation between these proteins (10% similarity at the amino acid level). However, both contain a C_3HC_4 RING finger [C-X_2-C-$X_{(9–39)}$-C-$X_{(1–3)}$-H-$X_{(2–3)}$-C-X_2-C-$X_{(4–48)}$-C-X_2-C] (3) close to the N terminus. A striking difference between these two proteins is the absence of the ICP0 C terminus in the sequence of ORF61p. Importantly, this region is required for targeting ICP0 to ND10 bodies and subsequently degrading their components (16, 18, 45). Therefore, we investigated the ability of ORF61p to mediate the degradation of PML and Sp100.

ORF61p is unable to efficiently degrade PML and Sp100. The effects of ORF61p and ICP0 on the localization of PML and Sp100 in MeWo cells transformed with plasmids encoding these two orthologs were monitored using immunofluorescence microscopy. In mock-treated cells, both PML and Sp100 appeared as punctate nuclear bodies (Fig. 2A and D) (2). As reported previously, the expression of ICP0 resulted in the disappearance of both cell proteins (Fig. 2B and E) (46). However, cells expressing ORF61p displayed a different phenotype. Although PML-containing bodies in these cells were more dispersed and smaller than those in mock-treated cells, PML was still detected, mostly in punctate intracellular structures (Fig. 2C). The effect of ORF61p on Sp100 seemed more similar to that of ICP0, as staining for Sp100 nuclear bodies disappeared from most cells expressing ORF61p (Fig. 2F).

To directly assay the effects of virus products on PML and Sp100 abundance, MeWo cells were mock treated or infected with replication-deficient adenoviruses expressing either no

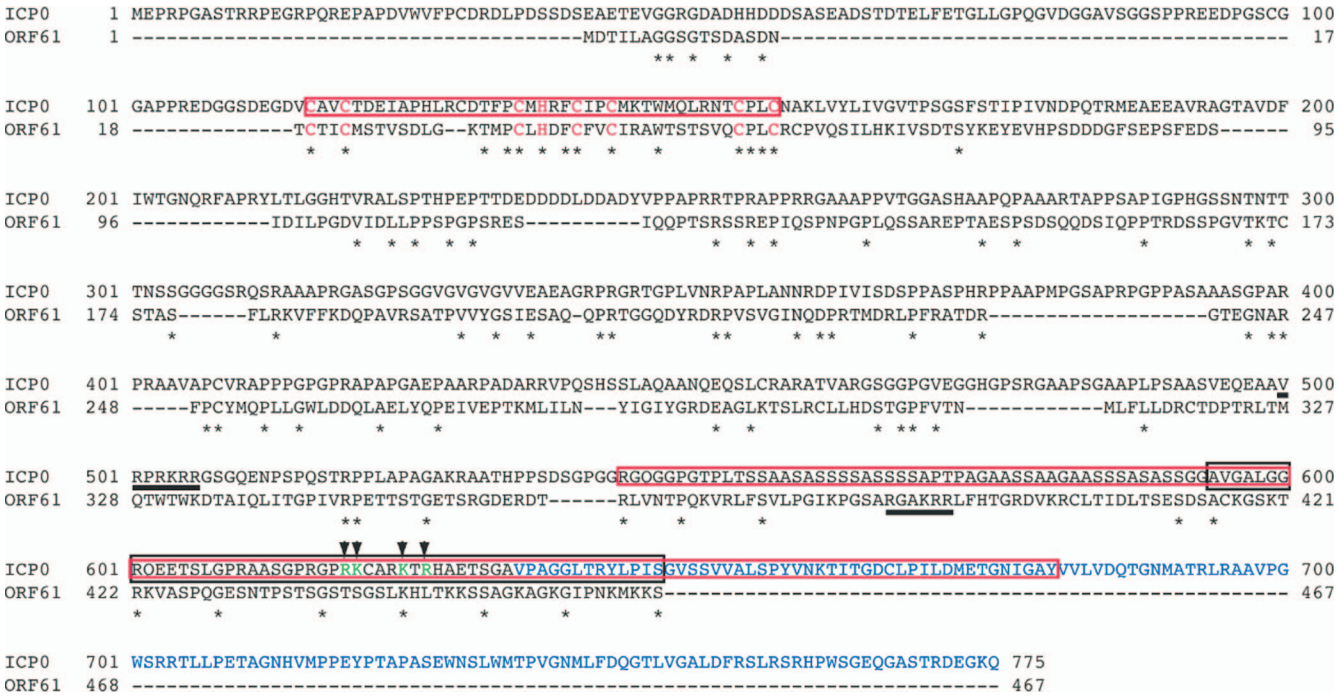

FIG. 1. Alignment of the amino acid sequences of ICP0 and ORF61p (NCBI protein database accession numbers NP_044601.1 and NP_040183.1, respectively) by using the Gonnet matrix, an open-gap penalty of 10.0, and an extend-gap penalty of 0.1. The Cys and His residues of the C_3HC_4 RING finger consensus sequence are shown in red. The ND10-targeting domain (18) in the C terminus of ICP0 is shown in blue. The nuclear localization signal regions of ICP0 and ORF61p are underlined (52, 63). The USP7 interaction site is marked with a black box, and the amino acids required for interaction are shown in green and identified by arrowheads (19). The two regions that encode E3 ubiquitin ligase activities (30) are marked with red boxes. Asterisks indicate identical residues.

herpesvirus proteins (Adempty), ICP0 (AdICP0), or ORF61p (AdORF61), and viral and cellular protein levels were monitored by Western blotting (Fig. 3). By using a multiplicity of infection (MOI) of 5, we ensured that every cell was infected and expressed the protein of interest. In mock-infected cells or cells infected with Adempty, PML appeared as a series of bands with different molecular masses. These bands represent alternatively spliced and posttranslationally modified forms of PML (54). Three predominant forms of Sp100 (Sp100A, Sp100A-SUMO, and Sp100-HMG) were detected as described previously (27, 66). ICP0 expression resulted in the complete disappearance of multiple PML isoforms and the preferential loss of the slower-migrating species of Sp100 (Fig. 3) (8). In contrast, the expression of ORF61p had no effect on the abundance or species of PML detected by this assay. ORF61p consistently reduced Sp100 levels, although not as efficiently as ICP0 (Fig. 3). Immunofluorescence analysis of cells infected in parallel verified that all cells were infected and expressed ICP0 or ORF61p (data not shown). PML in cells infected with Adempty was reorganized as elongated tracks, presumably in response to the expression of adenovirus E4 ORF3 (6). The expression of ICP0 by AdICP0 led to the loss of PML, whereas PML staining in AdORF61-infected cells was identical to that in the Adempty sample (data not shown). This observation further differentiates ICP0 from ORF61p.

Taken together, the immunofluorescence data and the Western blotting analysis demonstrate that ORF61p alters the integrity and the staining pattern of ND10 bodies. However, its expression does not result in the disappearance of PML but does affect Sp100 levels.

Targeting of ORF61p to ND10s does not cause PML degradation. As mentioned above, the C terminus of ICP0, which is required for targeting to ND10s and efficient degradation of PML (16, 18, 45), is absent from ORF61p (Fig. 1). The addition of this domain to β-galactosidase caused the partial colocalization of the fusion construct with PML (18). We asked if ORF61p's failure to decrease PML levels was a consequence of its inability to target ND10s because it lacked this domain. To test this possibility, a translational fusion of ORF61p with the C-terminal 188 aa of ICP0 was created (Fig. 4A). The resulting protein should contain all the regions of ICP0 required for PML targeting and degradation (a RING finger homologous to that of ICP0 and the ICP0 C-terminal targeting region) (16).

MeWo cells were either mock treated or transformed with constructs expressing ICP0, ORF61p, or the fusion protein. Western blot analysis of cell lysates revealed that all protein products accumulated at similar levels and that the addition of the C-terminal region of ICP0 did not alter ORF61p stability (Fig. 4B). The localization and abundance of these proteins and PML were then monitored. As described above, ICP0 expression led to the disappearance of PML staining whereas the expression of ORF61p resulted in only slight changes in the intracellular PML staining pattern (Fig. 2B and C). The fusion protein had a subcellular localization pattern distinct from that of ICP0 or ORF61p. In most cells (approximately 80 to 90%),

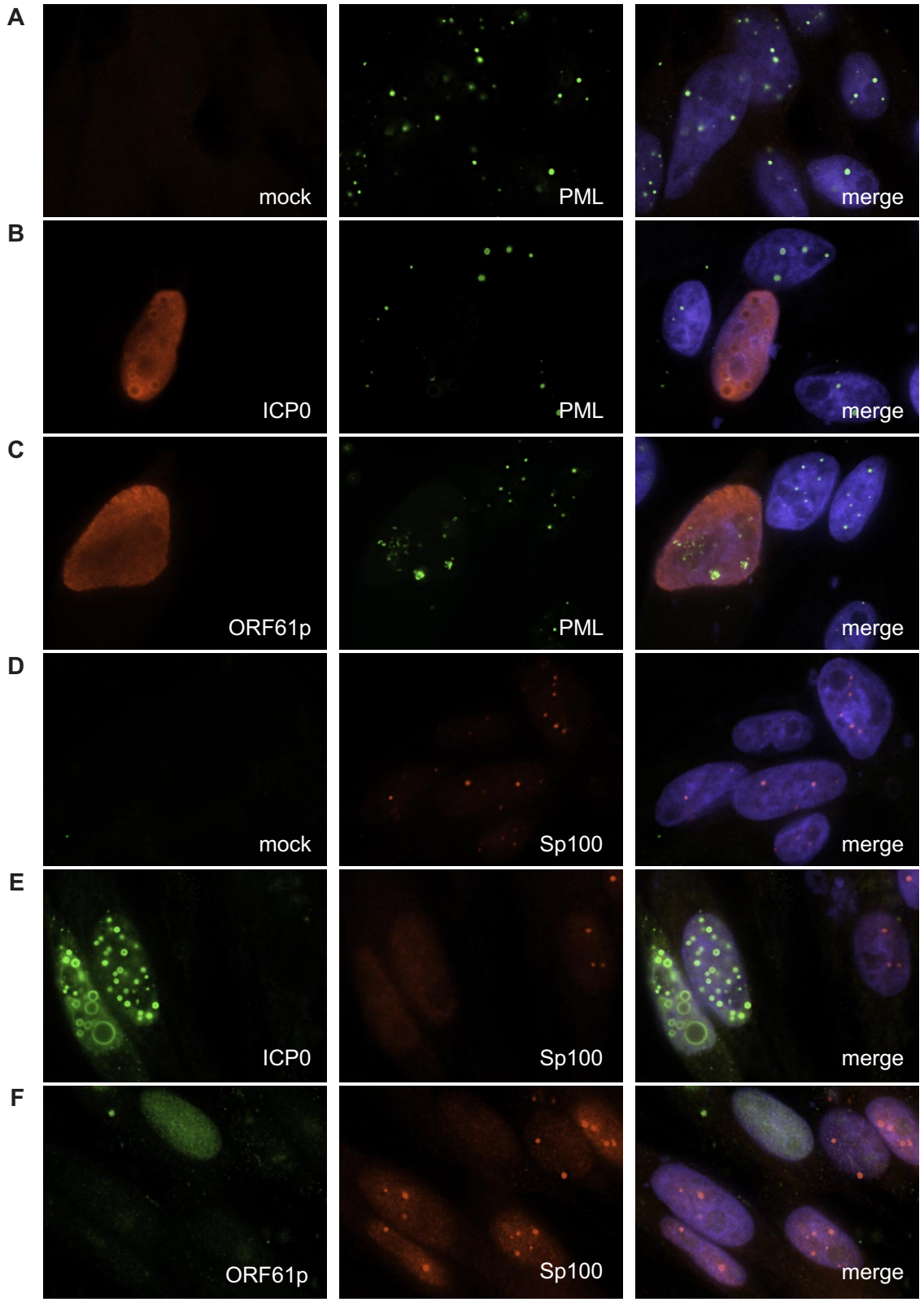

FIG. 2. Redistribution of PML and Sp100 in ICP0- or ORF61p-expressing cells. MeWo cells grown on glass coverslips were mock treated (A and D) or transformed with plasmid constructs expressing ICP0 (B and E) or ORF61p (C and F). Forty-eight hours posttransformation, cells were fixed and the localization of viral proteins and PML (A to C) or Sp100 (D to F) was monitored by indirect immunofluorescence microscopy. The nuclei were stained with Hoechst. Images were captured with a 100× objective and analyzed by volume deconvolution.

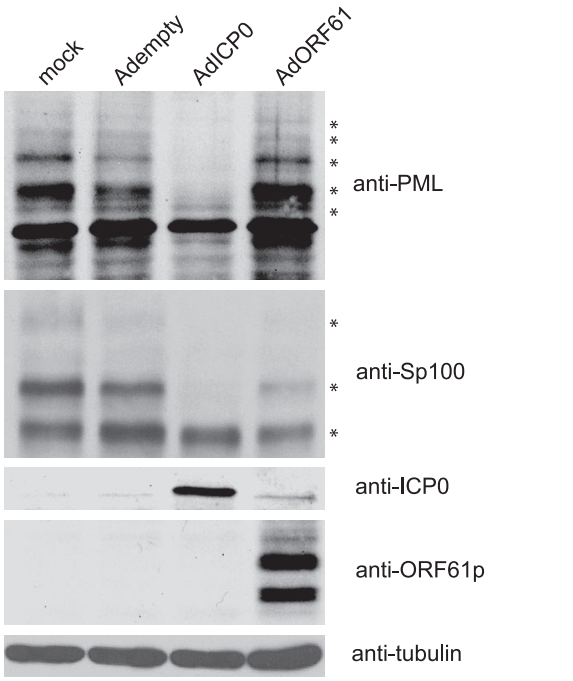

FIG. 3. Abundance of PML and Sp100 in ICP0- or ORF61p-expressing cells. MeWo cells were mock treated or infected with Adempty, AdICP0, or AdORF61 at an MOI of 5. Forty-eight hours postinfection, total cell lysates were analyzed by SDS-PAGE. The levels of PML, Sp100, ICP0, ORF61p, and tubulin were analyzed by Western blotting. The major species of PML and Sp100 are identified by asterisks.

the fusion protein was predominantly cytoplasmic (Fig. 4D). Similar to the β-galactosidase–ICP0 C-terminal domain fusion product (18), the ORF61p fusion protein colocalized with a subpopulation of cytoplasmic PML-containing bodies. In the 10 to 20% of the population in which the protein was nuclear, chromatin was displaced to the inner edges of the nuclear membrane and the fusion protein filled the remaining nuclear space (Fig. 4E). However, in both cases, although PML distribution was altered, PML was still detected. Thus, the failure of ORF61p to lower intracellular levels of PML is not because it lacks an ND10-targeting domain but rather is an intrinsic property of the protein.

Distribution and abundance of PML and Sp100 during VZV infection. ORF61p alone does not efficiently degrade PML and Sp100 (Fig. 2 and 3). We next asked if other VZV proteins affected the distribution of these proteins during infection. MeWo cells were infected with HSV or cell-free VZV, and the intracellular distribution of viral and cellular proteins was monitored by immunofluorescence microscopy. As reported previously, in cells infected with HSV, staining for PML and Sp100 disappears (Fig. 5A and 6A). During our initial analyses, staining for ORF61p was the marker for virus-infected cells. We noticed that in cells expressing ORF61p, PML-containing bodies appeared to be smaller and less bright than those in uninfected cells. However, unlike cells infected with HSV, VZV-infected cells still contained detectable PML (Fig. 5B). Nevertheless, because the expression kinetics of VZV-encoded proteins is not fully understood and it might be possible that other proteins expressed after ORF61p contribute to the loss of PML during infection, we used ORF62p as an alternative marker for infected cells. This protein initially localizes to the nuclei of infected cells; however, it is subsequently phosphorylated and translocates to the cytoplasm later in infection (11). Therefore, its intracellular localization pattern is useful as a marker of infected cells and as an indicator of the stage of the virus replication cycle. In cells in which ORF62p was nuclear, both PML and Sp100 appeared as spherical structures, very similar to what is seen in uninfected cells (Fig. 5C and 6B). Infected cells at late time points postinfection were monitored using staining for the glycoprotein gE. Late in VZV infection, the localization of ND10 components was similar to that observed in transformed cells (Fig. 2). Specifically, PML bodies were still present, although their abundance appeared to be decreased and their staining intensity was less than that seen in uninfected cells (Fig. 5D). In contrast, the characteristic punctate staining for Sp100 was not detected (Fig. 6C).

To further investigate the fate of ND10 components during VZV infection and quantitatively measure their abundance, we infected MeWo cells with either HSV or cell-free VZV and monitored virus and cell protein levels by Western blotting. As described previously, HSV infection results in the rapid degradation of multiple isoforms of PML and Sp100 (Fig. 7A) (8). VZV cell-free titers are low and the kinetics of virus replication is very slow compared to that of HSV. Therefore, to assay the effect of virus infection on these proteins, we monitored their levels for several days postinfection. In contrast to what occurs during HSV infection, levels of both PML and Sp100 increased during this period of observation (Fig. 7A). The rate of increase of PML and Sp100 was significantly higher than that of tubulin, indicating that the increase in the abundance of these proteins is not a result of cell growth and replication. To verify this, we monitored intracellular levels of Daxx, another constitutive component of ND10. Unlike those of PML and Sp100, the intracellular levels of Daxx remained almost constant during the course of observation (Fig. 7A).

Because PML and Sp100 are induced by interferon (25, 60), we asked if the expression of these proteins is sensitive to interferon in MeWo cells and what effect interferon has on Daxx. MeWo cells were treated with two different concentrations of alpha interferon. To verify that the interferon pathway is stimulated in MeWo cells, levels of STAT1 and STAT2 and their activated phosphorylated forms were monitored by Western blotting (Fig. 7B). As made evident by the increased abundance and phosphorylation of these signaling molecules, the interferon response is active in MeWo cells. We then measured the abundance of the three ND10 components and saw that although PML and Sp100 expression was induced, Daxx levels remained unaltered by interferon treatment (Fig. 7B).

These experiments suggest that increased levels of PML and Sp100 during VZV infection result from induction in the response to interferon secreted by infected cells and the failure of VZV to target these proteins for degradation.

Functions of PML, Sp100, and Daxx during VZV infection. ICP0-directed degradation of PML and Sp100 is beneficial for HSV replication (21, 22). Daxx restricts infection with human cytomegalovirus and adenoviruses (34, 68, 71). Because VZV does not efficiently reduce levels of ND10 components, we asked if the downregulation of these proteins altered VZV replication kinetics and yields.

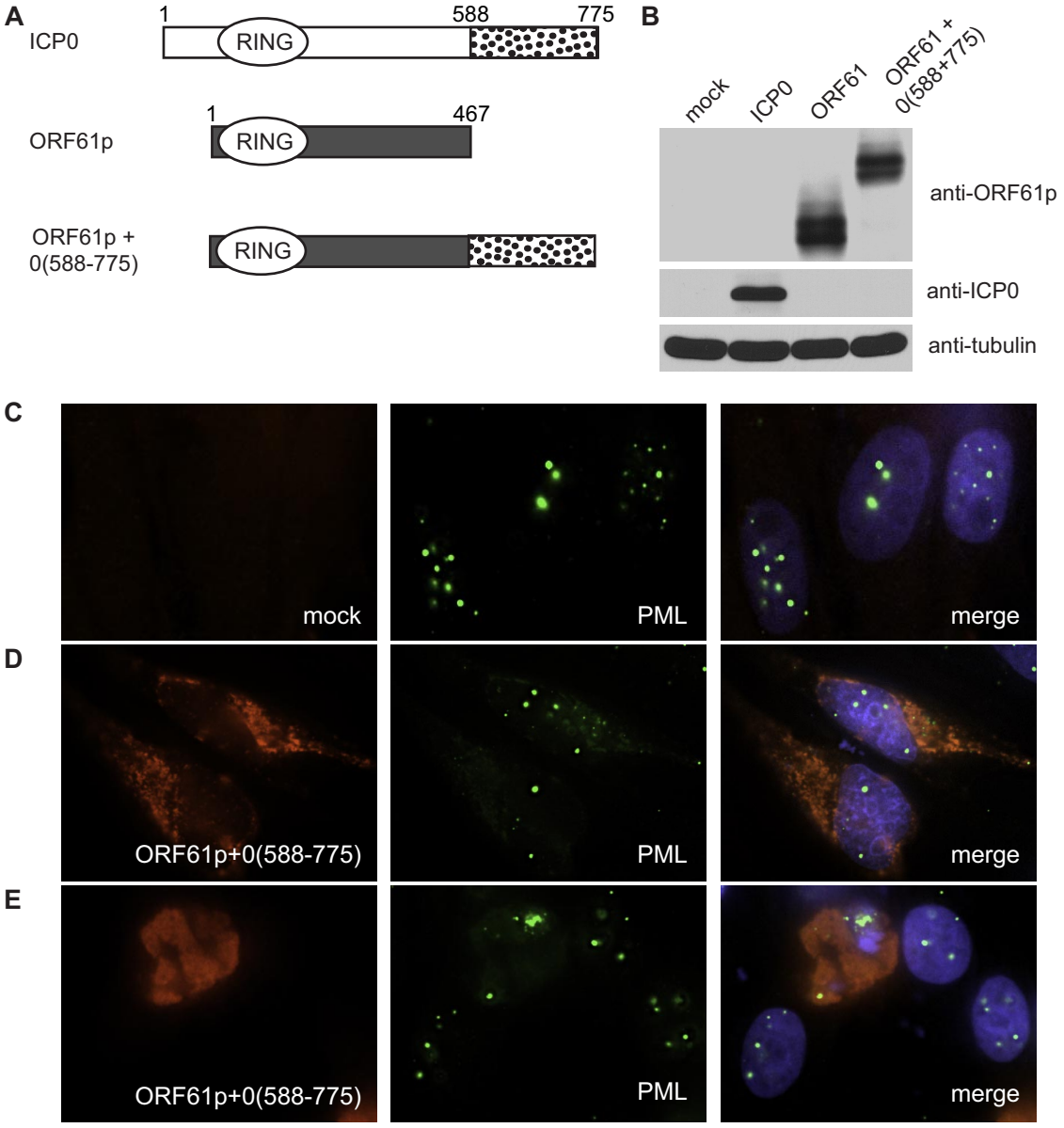

FIG. 4. Targeting of ORF61p to ND10s does not lead to PML degradation. (A) Schematic diagram of ICP0, ORF61p, and the ORF61p translational fusion with the C terminus of ICP0 [ORF61p + 0(588–775)]. (B) MeWo cells were mock treated or transformed with constructs expressing ICP0, ORF61p, or the ORF61p fusion protein. Forty-eight hours postinfection, total cell lysates were analyzed by SDS-PAGE. The levels of ICP0, ORF61p, and tubulin were analyzed by Western blotting. (C to E) MeWo cells grown on glass coverslips were mock treated (C) or transformed with plasmid constructs expressing the ORF61p fusion protein (D and E). After 48 h, cells were fixed and the localization patterns of ORF61p and PML were monitored by indirect immunofluorescence microscopy. Nuclei were stained with Hoechst. Images were captured with a 100× objective and analyzed by volume deconvolution.

Recombinant retroviruses expressing siRNAs targeting either nothing or PML, Sp100, or Daxx mRNA were used to transduce MeWo cells and generate stable cell lines (sicontrol, siPML, siSp100, and siDaxx, respectively). The abundance and localization of the targeted proteins in these cell lines were monitored by Western blotting (Fig. 8A) and immunofluorescence microscopy (data not shown). As previously reported (21, 22), the depletion of PML resulted in the loss of integrity of ND10 bodies and a change in the expression pattern of Sp100 but no significant difference in Daxx levels. In contrast, the downregulation of Sp100 or Daxx did not alter either the levels or the distribution of other ND10 components.

These cell lines were then used to measure VZV plaquing efficiency. Confluent monolayers were infected with serial dilutions of cell-free virus stocks. Several days postinfection, monolayers were fixed and stained and plaques were counted. The number of plaques formed on each cell line was normalized to the number formed on control cells. Our results revealed that when PML levels were reduced, the number of plaques increased by approximately 2.5-fold [$t_{(\mathrm{pval})} = 0.0017$,

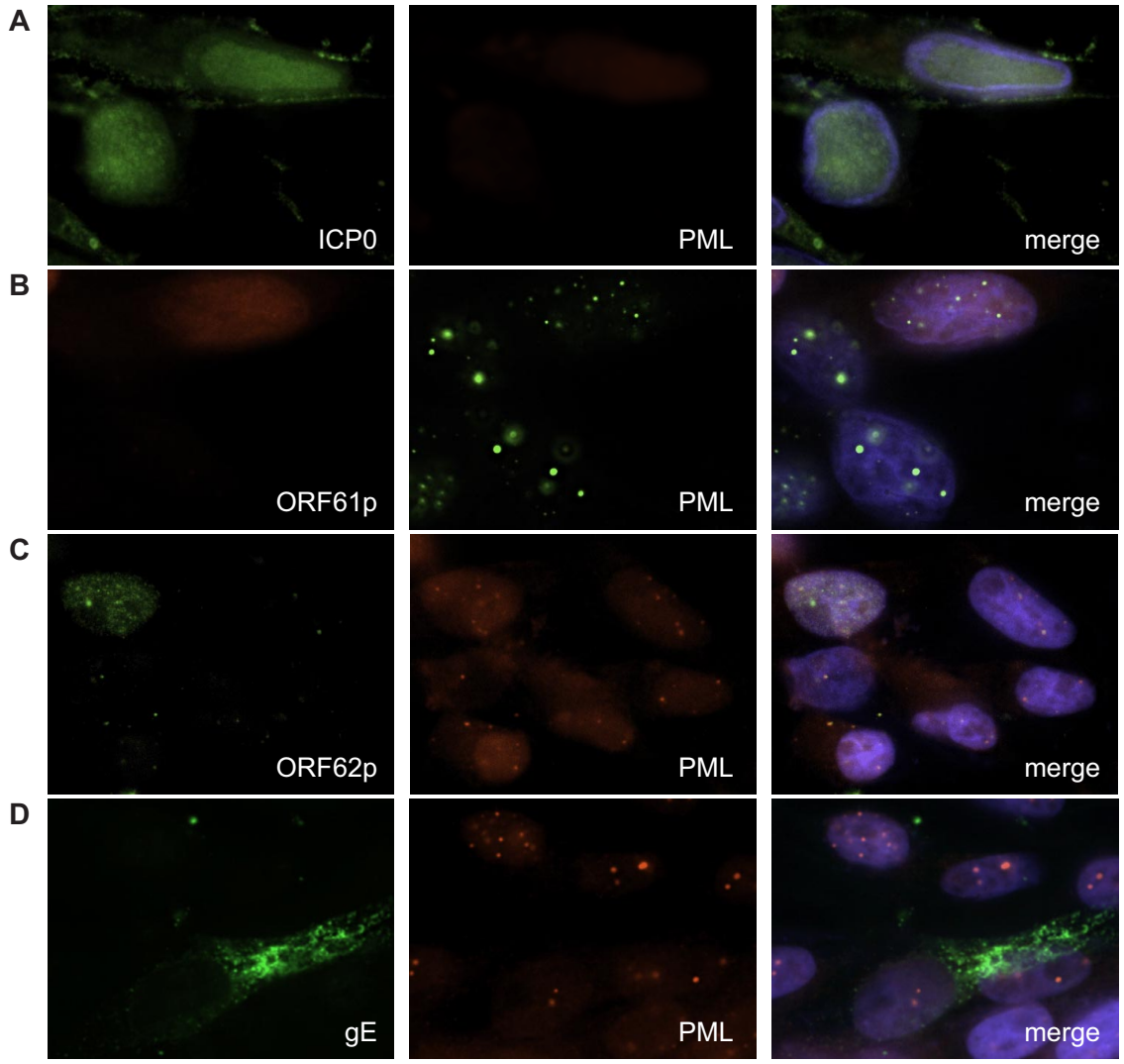

FIG. 5. Localization of PML during HSV and VZV infection. MeWo cells grown on glass coverslips were infected with HSV at an MOI of 1 (A) or cell-free VZV at an MOI of approximately 0.01 (B to D). HSV-infected cells were fixed at 6 hours postinfection (hpi), VZV-infected cells were fixed at 24 hpi, and the presence of ICP0 (A), ORF61p (B), ORF62p (C), gE (D), and PML (A to D) was monitored by indirect immunofluorescence microscopy. Nuclei were stained with Hoechst. Images were captured with a 100× objective and analyzed by volume deconvolution.

where pval is the *P* value] (Fig. 8B). This result mimics what is seen with an ICP0$^-$ mutant of HSV (22). In contrast, the downregulation of Sp100 resulted in a minor (1.2-fold) although consistent increase in the VZV titer [$t_{(\mathrm{pval})} = 0.031$] and the depletion of Daxx had no effect (Fig. 8B).

To further investigate the role of ND10 components in VZV growth, siRNA cell lines were infected with cell-free virus and the accumulation of virus proteins over time was monitored (Fig. 8C). Band intensities corresponding to virus proteins in each depleted cell line were normalized to what was present in control cells at the same time point. The intracellular levels of ORF63p, an immediate-early protein, and ORF29p, an early protein, were increased at early time points following the infection of siPML and siDaxx cells. However, at late times, the levels were similar to those in control cells. Like the plaquing efficiency results, the virus protein levels showed only a minor effect of the depletion of Sp100.

To study the formation of infectious centers, siRNA cell lines were infected with cell-free VZV and, at various times postinfection, cell-associated virus titers were measured. Consistent with the results of the Western analysis (Fig. 8C), the numbers of infectious centers formed in siPML and siDaxx cells increased early in infection before reaching a plateau, similar to those in sicontrol cells (Fig. 8D and E). The depletion of Sp100 had little influence on infectious-center yields (Fig. 8D and E).

We noticed that a cytopathic effect (CPE) was more pronounced in infected siPML cells than in infected cells of the other lines and that plaques were visible approximately 24 h earlier in siPML cells than in the other cells. In contrast, the plaque size in siDaxx monolayers was considerably smaller than those in the other cell lines and the virus-induced CPE was minimal, even at late times in infection. Furthermore, although the protein accumulation and infectious-center assays demonstrated accelerated

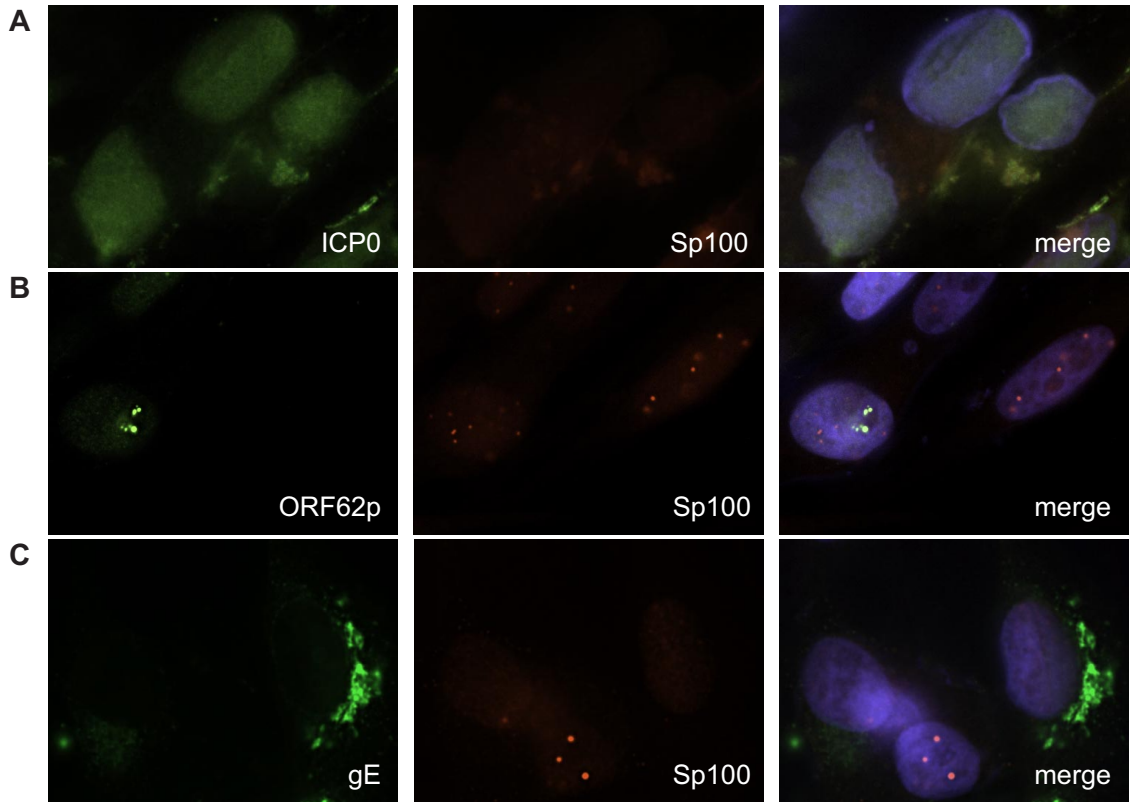

FIG. 6. Localization of Sp100 during HSV and VZV infection. MeWo cells grown on glass coverslips were infected with HSV at an MOI of 1 (A) or cell-free VZV at an MOI of approximately 0.01 (B and C). HSV-infected cells were fixed at 6 hpi, VZV-infected cells were fixed at 24 hpi, and the localization patterns of ICP0 (A), ORF62p (B), gE (C), and Sp100 (A to C) were monitored by indirect immunofluorescence microscopy. Nuclei were stained with Hoechst. Images were captured with a 100× objective and analyzed by volume deconvolution.

virus replication, similar to what occurred in siPML cells (Fig. 8C to E), we were surprised that the plaquing efficiency in siDaxx cells was identical to that in control cells (Fig. 8B). To probe the basis for these differences, siRNA cells grown on coverslips were infected and, at 2 and 3 days postinfection (dpi), cells were fixed and the expression of an immediate-early protein (ORF63p) and that of a late glycoprotein (gE) were monitored by immunofluorescence microscopy (Fig. 9). The nuclei of control cells at 2 dpi

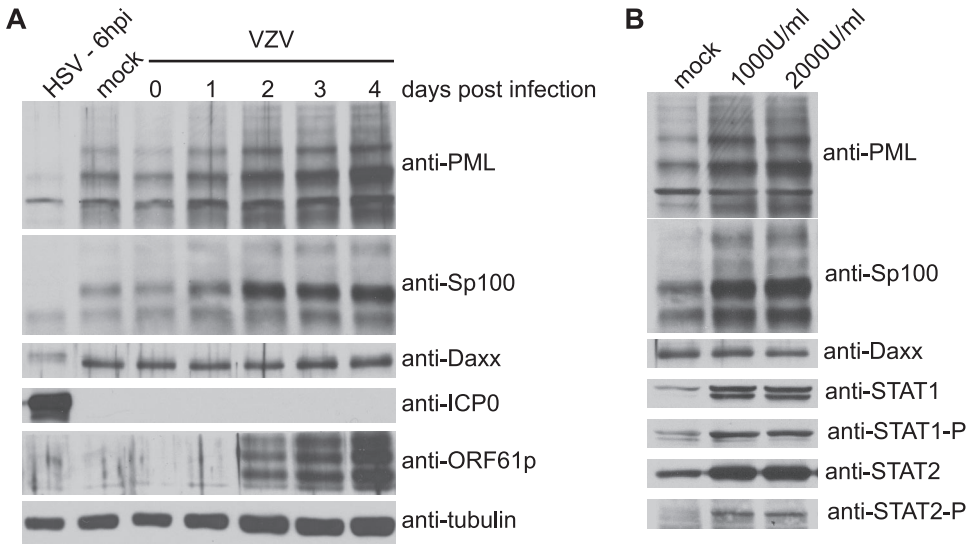

FIG. 7. Abundance of PML, Sp100, and Daxx during HSV and VZV infection. (A) MeWo cells were infected with HSV at an MOI of 5 or cell-free VZV at an MOI of approximately 0.01. At the indicated times postinfection, PML, Sp100, Daxx, ICP0, ORF61p, and tubulin levels were monitored by Western blotting. (B) MeWo cells were mock treated or incubated with medium containing 1,000 or 2,000 U/ml alpha interferon. Forty-eight hours posttreatment, total cell lysates were monitored for PML, Sp100, Daxx, STAT1, phosphorylated STAT1 (STAT1-P), STAT2, and phosphorylated STAT2 (STAT2-P).

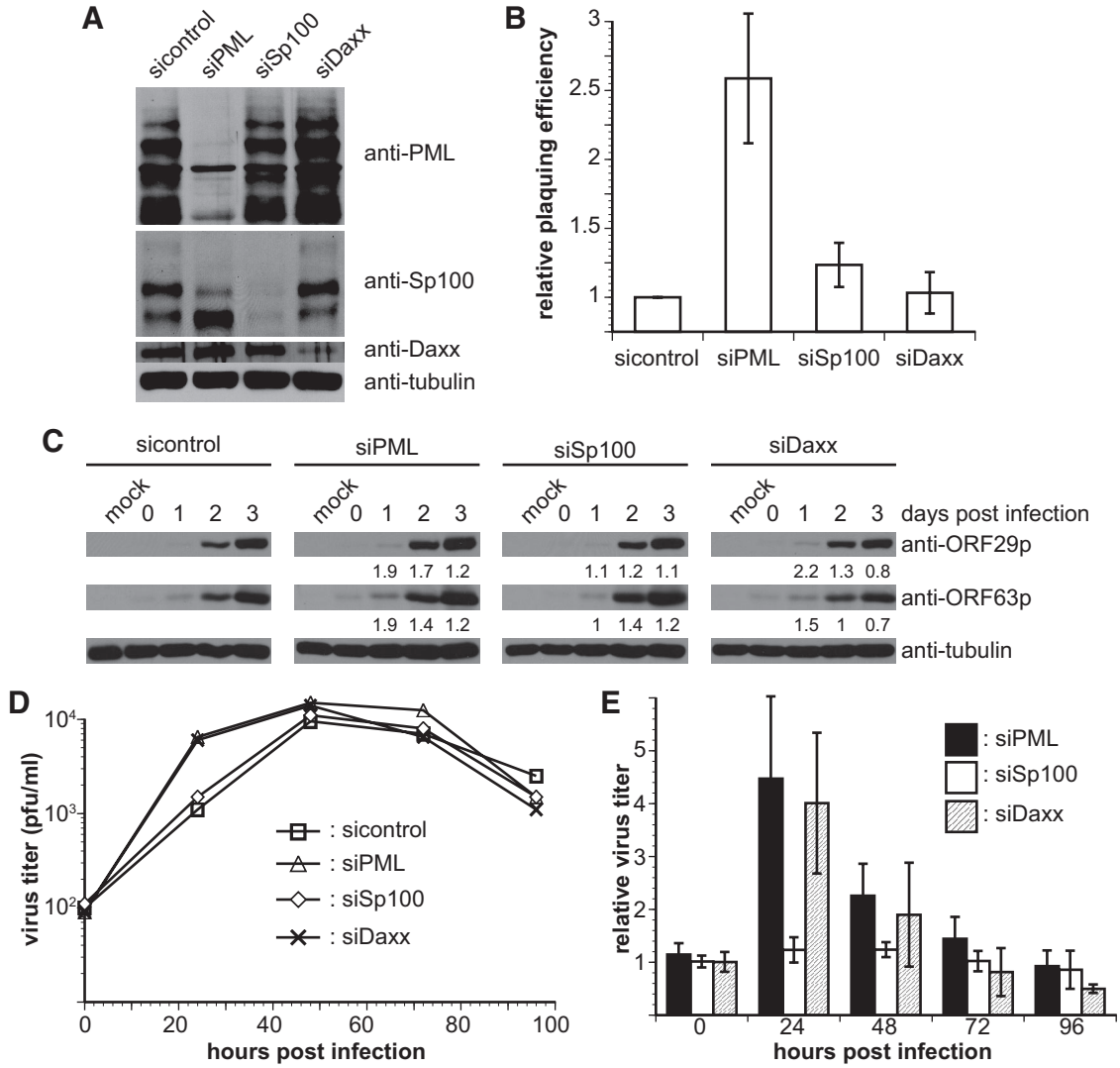

FIG. 8. Effects of PML, Sp100, and Daxx on VZV replication. (A) Total lysates from sicontrol, siPML, siSp100, and siDaxx cells were analyzed for PML, Sp100, Daxx, and tubulin levels by Western blotting. (B) sicontrol, siPML, siSp100, and siDaxx cells were infected with serial dilutions of VZV. Five days postinfection, monolayers were fixed and stained, plaques were counted, and the number was compared to the number formed in sicontrol cells. The error bars indicate standard deviations of results from five independent experiments, each performed in duplicate. (C) sicontrol, siPML, siSp100, and siDaxx cells were infected with cell-free VZV at an MOI of approximately 0.01. At the indicated times postinfection, lysates were analyzed for ORF29p, ORF63p, and tubulin by Western blotting. Band intensities were quantified using ImageJ and normalized to that for tubulin. The normalized quantities are listed below the appropriate lanes. (D) sicontrol, siPML, siSp100, and siDaxx cells were infected with cell-free VZV at an MOI of approximately 0.01. At the indicated times postinfection, cells were harvested and titrated to determine the number of infectious centers on fresh MeWo monolayers. Four days postinfection, monolayers were fixed and stained and plaques were counted to calculate the titers of infectious centers. Panel D shows the results of a representative experiment to determine the growth curve for VZV in each of the cell lines. Each datum point represents the average for two samples. Panel E displays the average of results for each time point from four independent experiments, and error bars represent standard deviations.

formed the characteristic ring-shaped structures that are indicative of cell fusion and efficient virus spread (37, 70). Infected foci in cells depleted of Sp100 were similar in size to those formed in sicontrol cells. VZV spread much faster in cells lacking PML or Daxx, as evidenced by the formation of larger foci in these cells at 2 dpi. However, unlike infection in siPML cells, in which extensive fusion occurred, infection in siDaxx cells spread with no apparent CPE. Moreover, at 2 dpi, cells were detached only from the siPML monolayer, resulting in holes that scored as plaques.

At 3 dpi (Fig. 9), CPEs on monolayers from all cell lines except siDaxx were obvious. Extensive cell fusion was detected, as evidenced by syncytium formation and the homogeneous staining patterns of viral proteins. The spread of infection in siDaxx cells was different from that in other cell lines. Although VZV spread to infect neighboring cells, individual intact infected cells without any evidence of cell fusion were detected. This morphology was strikingly different from that of sicontrol cells. Importantly, siDaxx cells were not detached even at this late stage in virus infection, which explains the considerably smaller plaque size. Importantly, because infected

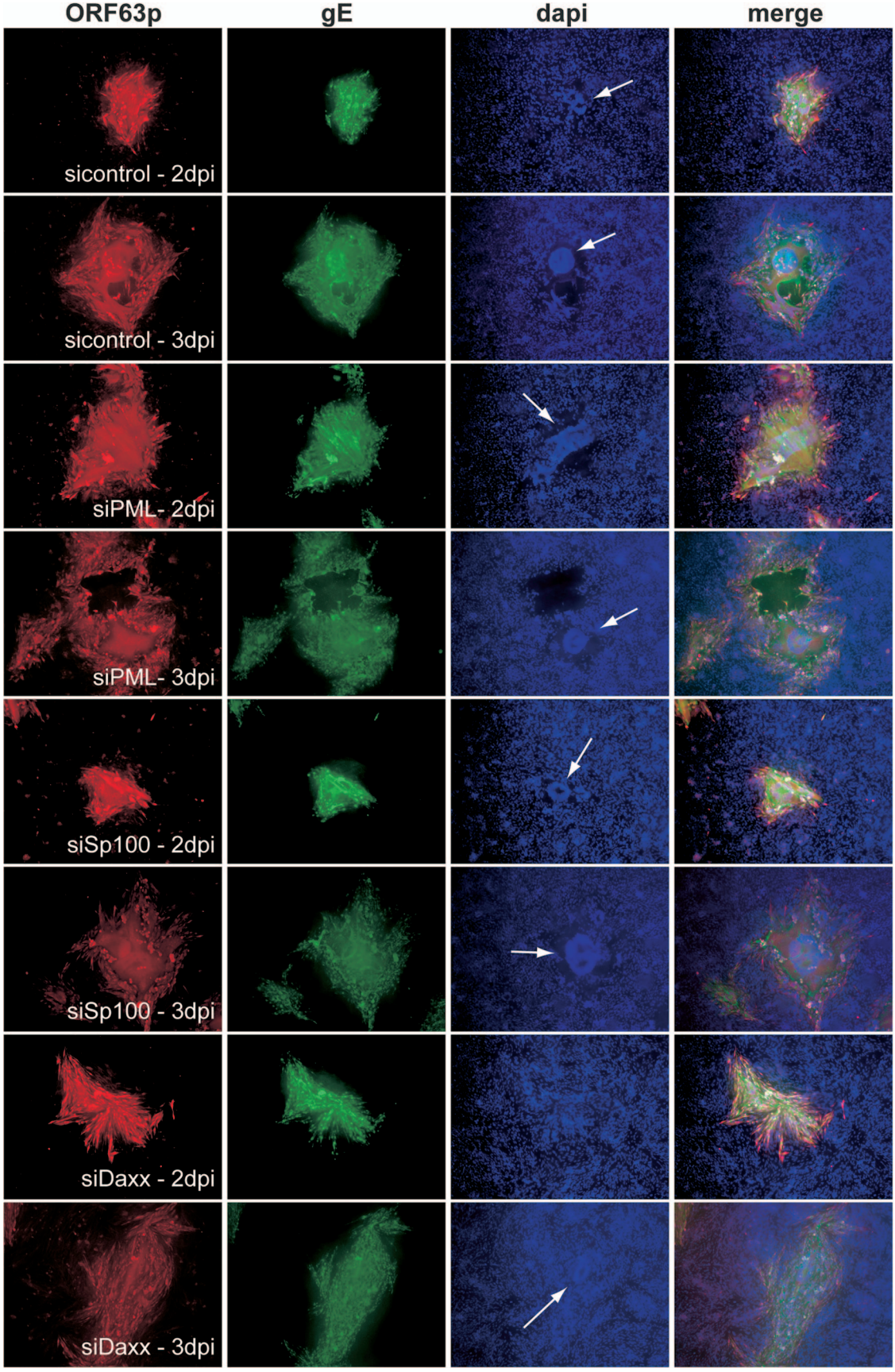

FIG. 9. Morphologies of infected foci on sicontrol, siPML, siSp100, and siDaxx cells. sicontrol, siPML, siSp100, and siDaxx cells were infected with cell-free VZV at an MOI of approximately 0.01. At 2 and 3 dpi, the cells were fixed and the localization patterns of ORF63p and gE were monitored by immunofluorescence microscopy. Nuclei were stained with Hoechst. Images were captured with a 10× objective. DAPI, 4′,6-diamidino-2-phenylindole.

siDaxx cells remained in the monolayer and failed to round up, they were often not scored as plaques, resulting in a seemingly lower level of plaquing efficiency (Fig. 8B).

This analysis of virus replication in cells lacking the major components of ND10 bodies demonstrated that PML is a repressor of wild-type VZV growth and that Sp100 has little if any role in this process. Daxx appeared to have a distinct function, because although the silencing of this protein initially resulted in accelerated replication and protein accumulation, virus-directed syncytium formation was defective.

DISCUSSION

Components of ND10 bodies, including PML, Sp100, and Daxx, associate with DNA virus genomes and contribute to an intrinsic antiviral mechanism that acts to repress expression from these genomes (10, 21, 22, 32, 35, 47, 67, 68). Herpesviruses have evolved countermeasures that bypass this cellular repression mechanism to ensure their efficient replication and spread. HSV encodes a potent transcriptional activator, ICP0, that targets ND10-associated proteins for proteasomal degradation, resulting in increased expression of immediate-early virus genes (21, 22).

VZV, a closely related alphaherpesvirus, encodes ORF61p, an ICP0 ortholog. Previous studies have emphasized the conservation of biological activities between these two proteins and demonstrated that both are activators of gene expression (49, 50). However, we previously showed that unlike ICP0, ORF61p fails to overcome a requirement for the cochaperone protein BAG3 during virus replication, suggesting that the orthologs have diverse functions (38).

The alignment of the amino acid sequences of these proteins revealed that while ORF61p retains the conserved RING finger residues of ICP0, it lacks the C terminus of its HSV ortholog (Fig. 1). Both of these regions are required for efficient targeting of ICP0 to ND10 bodies and the degradation of their components (16). The lack of the ICP0 C terminus and its associated ND10-targeting domain raised the possibility that ORF61p is unable to degrade components of PML bodies. Immunofluorescence analysis of cells transiently expressing ICP0 or ORF61p and Western blot analysis of proteins from cells infected with recombinant adenoviruses expressing the herpesvirus proteins revealed that ORF61p does not deplete PML and that Sp100 levels are decreased much less efficiently than those in cells expressing ICP0 (Fig. 3). Furthermore, attempts to target ORF61p to ND10 by the addition of the ICP0 targeting domain did not change this phenotype (Fig. 4).

Because ICP0 contains two separate E3 ubiquitin ligase activities, it has been described as a two-headed ubiquitin ligase (reviewed in reference 30) (Fig. 1). HSV ubiquitin ligase 1 (HUL-1) is encoded by ICP0 exon 3 and is responsible for the degradation of cdc34 (28, 29, 31). However, the HUL-2 activity that promotes the degradation of PML and Sp100 maps to the RING finger domain of ICP0 (4, 31). RING domains in the appropriate molecular context have been implicated in proteasomal degradation (42). Importantly, the binding of a ubiquitin protease (herpesvirus-associated ubiquitin-specific protease USP7) to the C terminus of ICP0 was suggested to promote the degradation of RING finger substrates (30). This binding may result in the sequestration of USP7 from newly ubiquitinated HUL-2 substrates and ensure their efficient targeting for proteasomal degradation (5, 20, 30).

Based on these observations, we envision two scenarios that explain why ORF61p does not cause the disappearance of PML and Sp100. Although the RING finger domain is required for its transcriptional activation activity (48), the molecular context of the rest of ORF61p may be inappropriate for it to act as an E3 ubiquitin ligase. Alternatively, the lack of a ubiquitin-specific protease binding site within ORF61p may lead to the availability of USP7, rapid deubiquitination of its targets, and thus protection from proteasomal degradation. We favor the latter hypothesis, as accumulating evidence in our laboratory suggests that unlike ICP0, which has self-preservation properties that depend on the binding of USP7 (5), ORF61p is rapidly degraded in a proteasome-dependent manner that requires a functional RING finger domain (C. A. Kyratsous, C. DeLong, and S. J. Silverstein, unpublished data). We infer from this observation that the RING finger of ORF61p possesses E3 ligase activity and can drive autoubiquitination but that the lack of a protease binding site results in ORF61p depletion. In support of this possibility, amino acids within the sequence of ICP0 that are required for the binding of USP7 (19) are not found in ORF61p (Fig. 1).

We further analyzed the relationship between VZV proteins and components of ND10s and observed that unlike PML and Sp100 levels during HSV infection, PML and Sp100 levels during VZV infection increase (Fig. 7A). This increase is specific for interferon-stimulated components of ND10s (Fig. 7B), as Daxx levels do not change throughout the course of infection (Fig. 7A). Because VZV induces interferon, we believe that virus proteins do not directly induce the synthesis of ND10 components and that, therefore, the increase in the abundance of PML and Sp100 is an indirect effect of interferon stimulation. We cannot exclude the possibility that other pathways not related to interferon may contribute to increased levels of PML and Sp100 in infected cells.

Surprisingly, although the autonomous expression of ORF61p results in decreased levels of Sp100 (Fig. 3), VZV infection results in an increase (Fig. 7). We posit that induction by interferon during infection masks the degradation of Sp100 by ORF61p. This effect contrasts with what is observed during HSV infection but remains consistent with our observation that ICP0 causes a more efficient decrease of Sp100 than ORF61p (Fig. 3).

HSV mutants lacking ICP0 are hypersensitive to interferon (51), and this effect is mediated by PML (7). Although VZV is sensitive to interferon, ORF61 mutants, unlike ICP0 mutants, are not hypersensitive to interferon (1). These data, along with our observation that PML is not degraded during VZV infection, suggest that interferon inhibits the replication of the two human alphaherpesviruses HSV and VZV through distinct mechanisms and that these viruses have evolved different and specific countermeasures. As a result, in contrast to HSV, VZV likely does not require the degradation of PML to overcome inhibition by interferon.

PML, Sp100, and Daxx were reported previously to suppress the early stages of herpesvirus replication (21, 22, 67, 68). Therefore, we asked if these proteins also affect the replication kinetics and yield of VZV. Stable cell lines depleted of each of these proteins were used for these analyses (Fig. 8A). In con-

trast to its role in HSV infection, Sp100 had little effect on the plaquing efficiency, gene expression, and infectious-center titers in cells infected with VZV. However, the infection of both siPML and siDaxx cell lines resulted in an increase in titer compared to those in the other cell lines and the accumulation of virus proteins at early times. Thus, PML and Daxx specifically inhibit the early stages of virus replication. Despite these differences, cell-associated titers of VZV in all cell lines reached the same peak at later times in infection. We posit that VZV replication is controlled by two independent host-mediated steps: an early block that is mediated by PML, Daxx, and possibly other host proteins and a late block that determines virus yield. Although the depletion of proteins that function early to inhibit the initial stages of the virus life cycle results in accelerated replication kinetics, it is not sufficient to increase the spread and development of infectious centers.

The function of ND10 components during wild-type HSV infection is difficult to study, as these proteins are rapidly degraded after ICP0 expression and are absent from infected cells. Thus, the depletion of these host products has no effect on wild-type virus replication kinetics and yield but enhances the replication of an ICP0$^-$ virus that fails to direct degradation (21, 22). Our results demonstrate that wild-type VZV mimics ICP0$^-$ virus replication in cells depleted of PML (Fig. 8) and fails to direct the degradation of the major component of ND10 bodies (Fig. 3). We have shown that, in contrast to the abundance of PML, the abundance of Sp100 is partially decreased when ORF61p is expressed (Fig. 3) and that the depletion of this protein has only a minor effect on virus replication (Fig. 8). Thus, VZV might have evolved to titrate Sp100 levels to the extent required for efficient replication. Alternatively, the small amounts of Sp100 remaining within the cells after siRNA depletion may be sufficient for it to silence VZV.

In conclusion, we have shown that VZV grown in cell culture behaves as a unique member of the alphaherpesvirus family. Unlike other ICP0 orthologs (55), ORF61p does not direct the degradation of ND10 components. VZV's interaction with this intrinsic defense mechanism is most similar to the way adenovirus deals with host-mediated silencing (71, 72). Neither virus is able to degrade ND10 proteins, and yet both overcome restriction by interferon. Moreover, in contrast to HSV replication but like adenovirus replication, VZV replication is unaffected by the depletion of Sp100 but is accelerated when PML and Daxx are silenced. Although HSV and VZV are considered to be very similar, this study demonstrates that they have evolved unique and specialized ways to interfere with host cell repression to ensure their efficient growth and spread.

ACKNOWLEDGMENTS

We thank Matthew Walters and Daniel Wolf for helpful discussions.

This study was supported by a grant from the Public Health Service, no. AI-024021, to S.J.S.

REFERENCES

1. **Ambagala, A. P., and J. I. Cohen.** 2007. Varicella-zoster virus IE63, a major viral latency protein, is required to inhibit the alpha interferon-induced antiviral response. J. Virol. **81:**7844–7851.
2. **Ascoli, C. A., and G. G. Maul.** 1991. Identification of a novel nuclear domain. J. Cell Biol. **112:**785–795.
3. **Borden, K. L., and P. S. Freemont.** 1996. The RING finger domain: a recent example of a sequence-structure family. Curr. Opin. Struct. Biol. **6:**395–401.
4. **Boutell, C., S. Sadis, and R. D. Everett.** 2002. Herpes simplex virus type 1 immediate-early protein ICP0 and its isolated RING finger domain act as ubiquitin E3 ligases in vitro. J. Virol. **76:**841–850.
5. **Canning, M., C. Boutell, J. Parkinson, and R. D. Everett.** 2004. A RING finger ubiquitin ligase is protected from autocatalyzed ubiquitination and degradation by binding to ubiquitin-specific protease USP7. J. Biol. Chem. **279:**38160–38168.
6. **Carvalho, T., J. S. Seeler, K. Ohman, P. Jordan, U. Pettersson, G. Akusjarvi, M. Carmo-Fonseca, and A. Dejean.** 1995. Targeting of adenovirus E1A and E4-ORF3 proteins to nuclear matrix-associated PML bodies. J. Cell Biol. **131:**45–56.
7. **Chee, A. V., P. Lopez, P. P. Pandolfi, and B. Roizman.** 2003. Promyelocytic leukemia protein mediates interferon-based anti-herpes simplex virus 1 effects. J. Virol. **77:**7101–7105.
8. **Chelbi-Alix, M. K., and H. de Thé.** 1999. Herpes virus induced proteasome-dependent degradation of the nuclear bodies-associated PML and Sp100 proteins. Oncogene **18:**935–941.
9. **Davison, A. J., and J. E. Scott.** 1986. The complete DNA sequence of varicella-zoster virus. J. Gen. Virol. **67:**1759–1816.
10. **Doucas, V., A. M. Ishov, A. Romo, H. Juguilon, M. D. Weitzman, R. M. Evans, and G. G. Maul.** 1996. Adenovirus replication is coupled with the dynamic properties of the PML nuclear structure. Genes Dev. **10:**196–207.
11. **Eisfeld, A. J., S. E. Turse, S. A. Jackson, E. C. Lerner, and P. R. Kinchington.** 2006. Phosphorylation of the varicella-zoster virus (VZV) major transcriptional regulatory protein IE62 by the VZV open reading frame 66 protein kinase. J. Virol. **80:**1710–1723.
12. **Everett, R. D.** 1985. Activation of cellular promoters during herpes virus infection of biochemically transformed cells. EMBO J. **4:**1973–1980.
13. **Everett, R. D.** 1989. Construction and characterization of herpes simplex virus type 1 mutants with defined lesions in immediate early gene 1. J. Gen. Virol. **70:**1185–1202.
14. **Everett, R. D.** 2006. Interactions between DNA viruses, ND10 and the DNA damage response. Cell. Microbiol. **8:**365–374.
15. **Everett, R. D., W. C. Earnshaw, J. Findlay, and P. Lomonte.** 1999. Specific destruction of kinetochore protein CENP-C and disruption of cell division by herpes simplex virus immediate-early protein Vmw110. EMBO J. **18:**1526–1538.
16. **Everett, R. D., P. Freemont, H. Saitoh, M. Dasso, A. Orr, M. Kathoria, and J. Parkinson.** 1998. The disruption of ND10 during herpes simplex virus infection correlates with the Vmw110- and proteasome-dependent loss of several PML isoforms. J. Virol. **72:**6581–6591.
17. **Everett, R. D., P. Lomonte, T. Sternsdorf, R. van Driel, and A. Orr.** 1999. Cell cycle regulation of PML modification and ND10 composition. J. Cell Sci. **112:**4581–4588.
18. **Everett, R. D., and G. G. Maul.** 1994. HSV-1 IE protein Vmw110 causes redistribution of PML. EMBO J. **13:**5062–5069.
19. **Everett, R. D., M. Meredith, and A. Orr.** 1999. The ability of herpes simplex virus type 1 immediate-early protein Vmw110 to bind to a ubiquitin-specific protease contributes to its roles in the activation of gene expression and stimulation of virus replication. J. Virol. **73:**417–426.
20. **Everett, R. D., M. Meredith, A. Orr, A. Cross, M. Kathoria, and J. Parkinson.** 1997. A novel ubiquitin-specific protease is dynamically associated with the PML nuclear domain and binds to a herpesvirus regulatory protein. EMBO J. **16:**566–577.
21. **Everett, R. D., C. Parada, P. Gripon, H. Sirma, and A. Orr.** 2008. Replication of ICP0-null mutant herpes simplex virus type 1 is restricted by both PML and Sp100. J. Virol. **82:**2661–2672.
22. **Everett, R. D., S. Rechter, P. Papior, N. Tavalai, T. Stamminger, and A. Orr.** 2006. PML contributes to a cellular mechanism of repression of herpes simplex virus type 1 infection that is inactivated by ICP0. J. Virol. **80:**7995–8005.
23. **Gelman, I. H., and S. Silverstein.** 1985. Identification of immediate early genes from herpes simplex virus that transactivate the virus thymidine kinase gene. Proc. Natl. Acad. Sci. USA **82:**5265–5269.
24. **Grose, C., and P. A. Brunel.** 1978. Varicella-zoster virus: isolation and propagation in human melanoma cells at 36 and 32°C. Infect. Immun. **19:**199–203.
25. **Grotzinger, T., T. Sternsdorf, K. Jensen, and H. Will.** 1996. Interferon-modulated expression of genes encoding the nuclear-dot-associated proteins Sp100 and promyelocytic leukemia protein (PML). Eur. J. Biochem. **238:**554–560.
26. **Gu, H., and B. Roizman.** 2003. The degradation of promyelocytic leukemia and Sp100 proteins by herpes simplex virus 1 is mediated by the ubiquitin-conjugating enzyme UbcH5a. Proc. Natl. Acad. Sci. USA **100:**8963–8968.
27. **Guldner, H. H., C. Szostecki, P. Schroder, U. Matschl, K. Jensen, C. Luders, H. Will, and T. Sternsdorf.** 1999. Splice variants of the nuclear dot-associated Sp100 protein contain homologies to HMG-1 and a human nuclear phosphoprotein-box motif. J. Cell Sci. **112:**733–747.
28. **Hagglund, R., and B. Roizman.** 2002. Characterization of the novel E3 ubiquitin ligase encoded in exon 3 of herpes simplex virus-1-infected cell protein 0. Proc. Natl. Acad. Sci. USA **99:**7889–7894.
29. **Hagglund, R., and B. Roizman.** 2003. Herpes simplex virus 1 mutant in which the ICP0 HUL-1 E3 ubiquitin ligase site is disrupted stabilizes cdc34 but

degrades D-type cyclins and exhibits diminished neurotoxicity. J. Virol. **77:** 13194–13202.
30. **Hagglund, R., and B. Roizman.** 2004. Role of ICP0 in the strategy of conquest of the host cell by herpes simplex virus 1. J. Virol. **78:**2169–2178.
31. **Hagglund, R., C. Van Sant, P. Lopez, and B. Roizman.** 2002. Herpes simplex virus 1-infected cell protein 0 contains two E3 ubiquitin ligase sites specific for different E2 ubiquitin-conjugating enzymes. Proc. Natl. Acad. Sci. USA **99:**631–636.
32. **Ishov, A. M., and G. G. Maul.** 1996. The periphery of nuclear domain 10 (ND10) as site of DNA virus deposition. J. Cell Biol. **134:**815–826.
33. **Ishov, A. M., R. M. Stenberg, and G. G. Maul.** 1997. Human cytomegalovirus immediate early interaction with host nuclear structures: definition of an immediate transcript environment. J. Cell Biol. **138:**5–16.
34. **Ishov, A. M., O. V. Vladimirova, and G. G. Maul.** 2002. Daxx-mediated accumulation of human cytomegalovirus tegument protein pp71 at ND10 facilitates initiation of viral infection at these nuclear domains. J. Virol. **76:**7705–7712.
35. **Jul-Larsen, A., T. Visted, B. O. Karlsen, C. H. Rinaldo, R. Bjerkvig, P. E. Lonning, and S. O. Boe.** 2004. PML-nuclear bodies accumulate DNA in response to polyomavirus BK and simian virus 40 replication. Exp. Cell Res. **298:**58–73.
36. **Koyama, K., and J. Osame.** March 2000. Stabilized live vaccine. U.S. patent 6039958.
37. **Kyratsous, C. A., and S. J. Silverstein.** 2007. BAG3, a host cochaperone, facilitates varicella-zoster virus replication. J. Virol. **81:**7491–7503.
38. **Kyratsous, C. A., and S. J. Silverstein.** 2008. The co-chaperone BAG3 regulates herpes simplex virus replication. Proc. Natl. Acad. Sci. USA **105:** 20912–20917.
39. **Laemmli, U. K.** 1970. Cleavage of structural proteins during the assembly of the head of bacteriophage T4. Nature **227:**680–685.
40. **Lium, E. K., C. A. Panagiotidis, X. Wen, and S. Silverstein.** 1996. Repression of the α0 gene by ICP4 during a productive herpes simplex virus infection. J. Virol. **70:**3488–3496.
41. **Lomonte, P., K. F. Sullivan, and R. D. Everett.** 2001. Degradation of nucleosome-associated centromeric histone H3-like protein CENP-A induced by herpes simplex virus type 1 protein ICP0. J. Biol. Chem. **276:**5829–5835.
42. **Lorick, K. L., J. P. Jensen, S. Fang, A. M. Ong, S. Hatakeyama, and A. M. Weissman.** 1999. RING fingers mediate ubiquitin-conjugating enzyme (E2)-dependent ubiquitination. Proc. Natl. Acad. Sci. USA **96:**11364–11369.
43. **Lungu, O., C. A. Panagiotidis, P. W. Annunziato, A. A. Gershon, and S. J. Silverstein.** 1998. Aberrant intracellular localization of varicella-zoster virus regulatory proteins during latency. Proc. Natl. Acad. Sci. USA **95:**7080–7085.
44. **Markowitz, D., S. Goff, and A. Bank.** 1988. A safe packaging line for gene transfer: separating viral genes on two different plasmids. J. Virol. **62:**1120–1124.
45. **Maul, G. G., and R. D. Everett.** 1994. The nuclear location of PML, a cellular member of the C3HC4 zinc-binding domain protein family, is rearranged during herpes simplex virus infection by the C3HC4 viral protein ICP0. J. Gen. Virol. **75:**1223–1233.
46. **Maul, G. G., H. H. Guldner, and J. G. Spivack.** 1993. Modification of discrete nuclear domains induced by herpes simplex virus type 1 immediate early gene 1 product (ICP0). J. Gen. Virol. **74:**2679–2690.
47. **Maul, G. G., A. M. Ishov, and R. D. Everett.** 1996. Nuclear domain 10 as preexisting potential replication start sites of herpes simplex virus type-1. Virology **217:**67–75.
48. **Moriuchi, H., M. Moriuchi, and J. I. Cohen.** 1994. The RING finger domain of the varicella-zoster virus open reading frame 61 protein is required for its transregulatory functions. Virology **205:**238–246.
49. **Moriuchi, H., M. Moriuchi, H. A. Smith, S. E. Straus, and J. I. Cohen.** 1992. Varicella-zoster virus open reading frame 61 protein is functionally homologous to herpes simplex virus type 1 ICP0. J. Virol. **66:**7303–7308.
50. **Moriuchi, H., M. Moriuchi, S. E. Straus, and J. I. Cohen.** 1993. Varicella-zoster virus (VZV) open reading frame 61 protein transactivates VZV gene promoters and enhances the infectivity of VZV DNA. J. Virol. **67:**4290–4295.
51. **Mossman, K. L., H. A. Saffran, and J. R. Smiley.** 2000. Herpes simplex virus ICP0 mutants are hypersensitive to interferon. J. Virol. **74:**2052–2056.
52. **Mullen, M. A., D. M. Ciufo, and G. S. Hayward.** 1994. Mapping of intracellular localization domains and evidence for colocalization interactions between the IE110 and IE175 nuclear transactivator proteins of herpes simplex virus. J. Virol. **68:**3250–3266.
53. **Muller, S., and A. Dejean.** 1999. Viral immediate-early proteins abrogate the modification by SUMO-1 of PML and Sp100 proteins, correlating with nuclear body disruption. J. Virol. **73:**5137–5143.
54. **Nisole, S., J. P. Stoye, and A. Saïb.** 2005. TRIM family proteins: retroviral restriction and antiviral defence. Nat. Rev. Microbiol. **3:**799–808.
55. **Parkinson, J., and R. D. Everett.** 2000. Alphaherpesvirus proteins related to herpes simplex virus type 1 ICP0 affect cellular structures and proteins. J. Virol. **74:**10006–10017.
56. **Pereira, L., M. H. Wolff, M. Fenwick, and B. Roizman.** 1977. Regulation of herpesvirus macromolecular synthesis. V. Properties of alpha polypeptides made in HSV-1 and HSV-2 infected cells. Virology **77:**733–749.
57. **Perry, L. J., F. J. Rixon, R. D. Everett, M. C. Frame, and D. J. McGeoch.** 1986. Characterization of the IE110 gene of herpes simplex virus type 1. J. Gen. Virol. **67:**2365–2380.
58. **Provost, P. J., D. L. Krah, and P. A. Friedman.** March 1997. Process for attenuated varicella zoster virus vaccine production. U.S. patent 5607852.
59. **Quinlan, M. P., and D. M. Knipe.** 1985. Stimulation of expression of a herpes simplex virus DNA-binding protein by two viral functions. Mol. Cell. Biol. **5:**957–963.
60. **Regad, T., and M. K. Chelbi-Alix.** 2001. Role and fate of PML nuclear bodies in response to interferon and viral infections. Oncogene **20:**7274–7286.
61. **Sourvinos, G., and R. D. Everett.** 2002. Visualization of parental HSV-1 genomes and replication compartments in association with ND10 in live infected cells. EMBO J. **21:**4989–4997.
62. **Sternsdorf, T., T. Grotzinger, K. Jensen, and H. Will.** 1997. Nuclear dots: actors on many stages. Immunobiology **198:**307–331.
63. **Stevenson, D., K. L. Colman, and A. J. Davison.** 1994. Delineation of a sequence required for nuclear localization of the protein encoded by varicella-zoster virus gene 61. J. Gen. Virol. **75:**3229–3233.
64. **Stow, N. D., and E. C. Stow.** 1986. Isolation and characterization of a herpes simplex virus type 1 mutant containing a deletion within the gene encoding the immediate early polypeptide Vmw110. J. Gen. Virol. **67:**2571–2585.
65. **Stuurman, N., A. de Graaf, A. Floore, A. Josso, B. Humbel, L. de Jong, and R. van Driel.** 1992. A monoclonal antibody recognizing nuclear matrix-associated nuclear bodies. J. Cell Sci. **101:**773–784.
66. **Szostecki, C., H. H. Guldner, H. J. Netter, and H. Will.** 1990. Isolation and characterization of cDNA encoding a human nuclear antigen predominantly recognized by autoantibodies from patients with primary biliary cirrhosis. J. Immunol. **145:**4338–4347.
67. **Tavalai, N., P. Papior, S. Rechter, M. Leis, and T. Stamminger.** 2006. Evidence for a role of the cellular ND10 protein PML in mediating intrinsic immunity against human cytomegalovirus infections. J. Virol. **80:**8006–8018.
68. **Tavalai, N., P. Papior, S. Rechter, and T. Stamminger.** 2008. Nuclear domain 10 components promyelocytic leukemia protein and hDaxx independently contribute to an intrinsic antiviral defense against human cytomegalovirus infection. J. Virol. **82:**126–137.
69. **Tavalai, N., and T. Stamminger.** 2008. New insights into the role of the subnuclear structure ND10 for viral infection. Biochim. Biophys. Acta **1783:** 2207–2221.
70. **Tzanck, A.** 1947. Le cytodiagnostic immediat en dermatologie. Bull. Soc. Fr. Dermatol. Syphiligr. **7:**68.
71. **Ullman, A. J., and P. Hearing.** 2008. Cellular proteins PML and Daxx mediate an innate antiviral defense antagonized by the adenovirus E4 ORF3 protein. J. Virol. **82:**7325–7335.
72. **Ullman, A. J., N. C. Reich, and P. Hearing.** 2007. Adenovirus E4 ORF3 protein inhibits the interferon-mediated antiviral response. J. Virol. **81:**4744–4752.
73. **Walters, M. S., C. A. Kyratsous, S. Wan, and S. Silverstein.** 2008. Nuclear import of the varicella-zoster virus latency-associated protein ORF63 in primary neurons requires expression of the lytic protein ORF61 and occurs in a proteasome-dependent manner. J. Virol. **82:**8673–8686.
74. **Yee, J. K., A. Miyanohara, P. LaPorte, K. Bouic, J. C. Burns, and T. Friedmann.** 1994. A general method for the generation of high-titer, pantropic retroviral vectors: highly efficient infection of primary hepatocytes. Proc. Natl. Acad. Sci. USA **91:**9564–9568.
75. **Zhu, X. X., C. S. Young, and S. Silverstein.** 1988. Adenovirus vector expressing functional herpes simplex virus ICP0. J. Virol. **62:**4544–4553.